Author's Accepted Manuscript

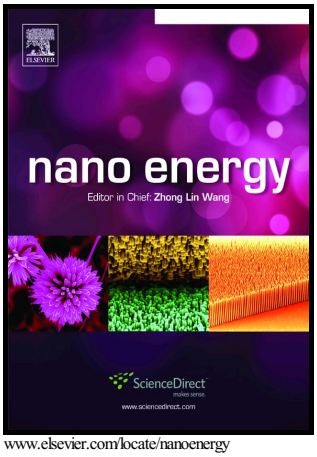

A brief review of sound energy harvesting

Jaehoon Choi, Inki Jung, Chong-Yun Kang

www.elsevier.com/locate/nanoenergy

PII: S2211-2855(18)30844-9
DOI: https://doi.org/10.1016/j.nanoen.2018.11.036
Reference: NANOEN3192

To appear in: *Nano Energy*

Received date: 1 October 2018
Revised date: 7 November 2018
Accepted date: 14 November 2018

Cite this article as: Jaehoon Choi, Inki Jung and Chong-Yun Kang, A brief review of sound energy harvesting, *Nano Energy,* https://doi.org/10.1016/j.nanoen.2018.11.036

A brief review of sound energy harvesting

Jaehoon Choi[a,b1], Inki Jung[a,b1], Chong-Yun Kang[a,b*]

[a]KU-KIST Graduate School of Converging Science and Technology, Korea University, Seoul 02841, Republic of Korea

[b]Center for Electronic Materials, Korea Institute of Science and Technology (KIST), Seoul 02792, Republic of Korea

[*]Correspondence should be addressed to cykang@kist.re.kr

Abstract

Sound energy harvesting is one of the promising technologies due to the abundant and clean sound sources. It can be the semi-permanent alternative power supplies for wireless sensor networks (WSNs), which is significant in the Internet of Things (IoT). However, sound waves have the low energy density, so there are many kinds of research in recent years to overcome this problem. This paper provides a comprehensive review of sound energy harvesting, focusing on presenting principles, examples and enhancement methods of sound energy harvesters. In this paper, various approaches are introduced which are classified as sound pressure amplification and transduction mechanism. For sound pressure amplification, two typical types of energy harvesters are presented that one is using a resonator, another one is using an acoustic metamaterial, and these are based on piezoelectric, electromagnetic, and triboelectric mechanisms to convert sound energy to electrical energy.

[1] These authors contributed equally to this work.

Graphical Abstract

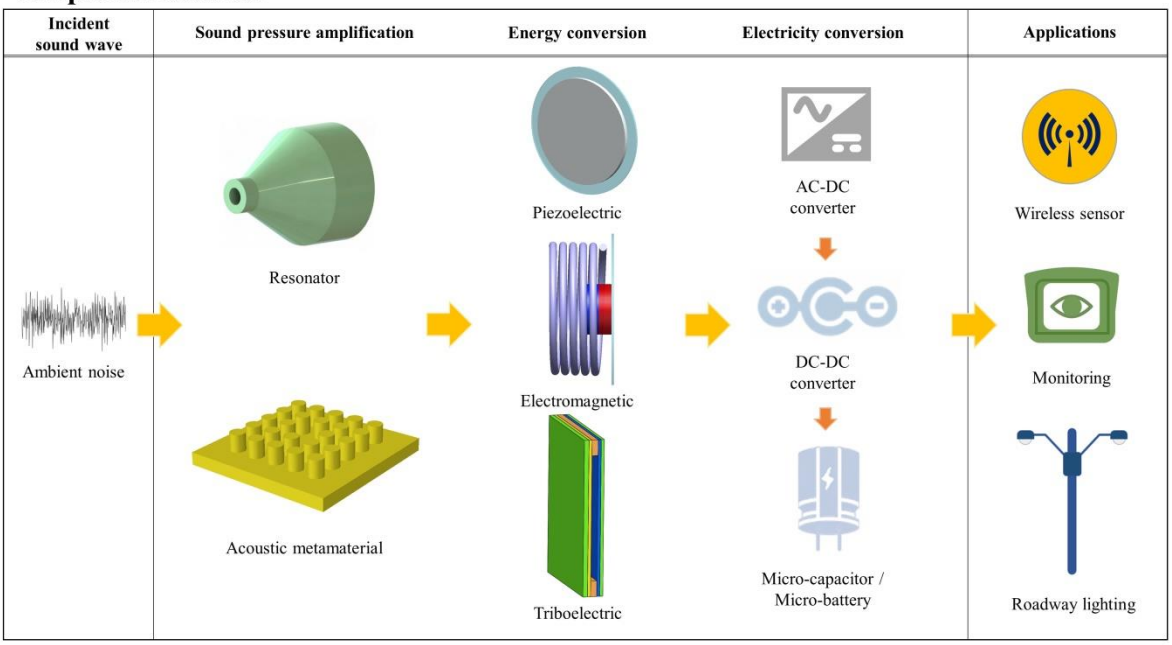

1. Introduction

Recently, we are entering the Internet of Things (IoT) era [1-3]. In the IoT system, one of the important things is that wireless sensor networks (WSNs) consist of numerous sensing devices to collect data and communicate with each other [1]. A large number of sensors such as temperature sensors [4], proximity sensors [5], ultrasonic sensors [6], or gas sensors [7,8] are widely distributed in the IoT system, and these can be operated by power source wired or wireless. Especially, in particular cite where access to power is difficult, batteries have been installed as wireless power source for WSNs. However, these batteries have a limited lifetime and require periodic replacement [9]. So, batteries cannot be suitable for some cases such as biomedical devices [10], environmental or industrial monitoring [11-13] and military applications [14-15]. Therefore, people have been getting interests in energy harvesting for WSNs and other applications [16]. Energy harvesting is the technology that converts ambient energy into useful energy such as electricity. Among various kinds of ambient energies such as motion [17,18], vibration or sound [19], thermal [20], wind [21] and solar energy [22,23], sound energy sources have a great potential for energy harvesting due to its abundance and cleanness. However, sound based energy harvesting methods are less studied than using the

other energy sources because of its low energy density. To overcome the low energy density of sound, various approaches are being conducted all over the world.

Sound energy harvesting technology is graphically expressed in Fig. 1. First, an ambient sound wave is collected and amplified by resonator or acoustic metamaterial, and it is converted into electrical energy by a specific energy conversion method. Lastly, rectification, regulation, and energy storage processes are executed for power electronics applications because the electrical energy appears in the form of alternating current (AC).

Fig. 1. Schematic of sound energy harvesting.

Since energy requirements are getting lower like WSNs and sound energy harvesting performance can be increased by proper harvester design, sound energy harvesting has a great potential to be used in certain applications such as providing energy to low power consumption devices and also it can solve the noise problem. In sound energy harvesting, audible frequency range (20 ~ 20,000 Hz) and low frequency sound (< 500 Hz) are useful because low frequency noise is mainly dominant and it is hard to block, which means it transmits well [24,25]. Different sound energy sources and its sound pressure level (SPL) are listed in Table 1. Sound pressure level is a logarithmic expression of the pressure of a sound relative to a reference value, and it is defined by

$$\mathrm{SPL} = 10\log_{10}\left(\frac{p}{p_0}\right)^2 = 20\log_{10}\frac{p}{p_0}\ (dB) \quad (1)$$

where p is the root mean square sound pressure, p_0 is the reference value (20 μPa) [26].

This paper is organized into three sections including this introduction. Section two is about the basics of sound energy harvesters and state-of-the-art sound energy harvesting techniques. Summary of this paper is presented in the last section.

Table 1. Sound pressure level of various sound sources.

2. Examples of sound energy harvesters

2.1 Basics of sound energy harvesters

Typical sound energy harvesters usually consist of resonator, membrane and piezoelectric material, which are shown in Fig. 2.

Fig. 2. Schematic of typical sound energy harvester.

Resonator produces sound oscillation at its resonant frequency. A membrane that one side attached to a resonator and another attached to a piezoelectric material oscillates together by sound oscillation. Piezoelectric material converts the mechanical energy into electrical energy. Resonators are generally used in sound energy harvesters to amplify the incident sound pressure because of its low energy density. There are three types in resonators, Helmholtz resonator, quarter-wavelength resonator, and half-wavelength resonator. In most applications, Helmholtz resonator [27-29] and quarter-wavelength resonator [30,31] are used. Helmholtz resonator is a large volume cavity connected with the outside space through a narrow neck as shown in Fig. 3(a). The resonant frequency of Helmholtz resonator is given by

$$f = \frac{c}{2\pi}\sqrt{\frac{A}{(l+\Delta l)V}} \qquad (2)$$

where c is the speed of sound, V is the volume of the cavity, l is the length of the neck, A is the cross-sectional area of the neck and Δl is the neck's end correction length [32].

Fig. 3. Schematic of resonators. (a) Helmholtz resonator. (b) Half wavelength tube resonator. (c) Quarter wavelength tube resonator.

As you can see in Fig. 3(b) and 3(c), a quarter-wavelength resonator has each open and closed end while a half-wavelength resonator has both open ends. The fundamental resonant frequency of a quarter-wavelength resonator and a half-wavelength resonator are given by equation (3) and (4), they are only related to the length of the resonator L, except the speed of sound c.

$$f = \frac{c}{4L} \text{ (quarter-wavelength resonator)} \quad (3)$$

$$f = \frac{c}{2L} \text{ (half-wavelength resonator)} \qquad (4)$$

A quarter-wavelength resonator can be thought as a Helmholtz resonator that one-third of tube length near the open end serves as a neck, and the remaining portion of the tube behaves like a cavity [33]. According to Sohn *et al*, a quarter-wavelength resonator has more than two times larger maximum sound absorption coefficient than half-wavelength resonator at the same tuning frequency of 560 Hz and design parameters. For the same volume, a quarter-wavelength resonator has a larger maximum sound absorption coefficient compared to Helmholtz resonator [34]. So, the quarter-wavelength resonator regards as the best resonator among the three types to collect sound energy at a given incident wave frequency.

2.2 Resonator based sound energy harvesters

Resonator based sound energy harvesters can be classified by energy conversion method such as piezoelectric, electromagnetic, and triboelectric. Most of the resonator based sound energy harvesters are the piezoelectric type. In other words, piezoelectric sound energy harvesters are most common and fundamental design. Horowitz *et al* made the first micro-scale sound energy harvester that consists of a Helmholtz resonator with a piezoelectric diaphragm [35]. The piezoelectric diaphragm has a silicon substrate layer, a TiO_2 layer and a PZT ring-shaped layer with top and bottom Pt electrodes. This piezoelectric diaphragm and two electrodes are fabricated on a silicon-on-insulator (SOI) wafers, and it is bonded to the Helmholtz resonator. The device is packed to fabricate a micro-scale sound energy harvester chip. This device's maximum output power for an optimal load of 982.9Ω was 6 pW with a power density of 0.34 μW/cm^2 at its resonant frequencies 13.568 kHz and incident sound pressure level 149 dB.

Li *et al* made the PZT piezoelectric beam array using a quarter-wavelength resonator [30,36]. First, they simulated and tested the single piezoelectric beam that moved inside the resonator from the open inlet to closed end for checking the harvested power output change at the first resonant frequency. It is reported that when the piezoelectric beam moves closer to the inlet, power output is higher due to the higher pressure gradient. However, in case of a single piezoelectric beam without the quarter-wavelength resonator, harvested voltage and power are just 0.038 V and 0.313 μW, while a single piezoelectric beam placed near the open inlet of the quarter-wavelength resonator harvests 1.51 V and 0.498 mW. This result shows

the effect of a quarter-wavelength resonator. Another experiment shows that the number of the piezoelectric beam to generate more power is optimized due to disturbance of air motion. Furthermore, it shows that the piezoelectric beams located in the first half of the resonator generate more power than the piezoelectric beams placed along the tube. The piezoelectric beam array using a quarter-wavelength resonator had the maximum voltage of 5.089 V and maximum power of 1.148 mW under the 100 dB SPL. Moreover, at 110 dB SPL, it generated 15.689 V and 12.697 mW, which is one of the highest harvested power above sound energy harvesters.

Similarly, Li *et al* used the PVDF piezoelectric beam array instead of PZT [31]. One thing different from the previous study is that there are two different types of beam array configuration. The first type is an aligned type that PVDF beams are in straight lines and the second type is a zigzag type. From the Fig. 4, the zigzag type generates more power than the aligned type because of reduced interference between the beams and air motion. The maximum voltage and power are 0.696 V and 0.31 μW when the PVDF beams are located in the first half of the quarter-wavelength resonator in the zigzag pattern at 100 dB SPL. Moreover, at 110 dB SPL, it generates 1.48 V and 2.2 μW.

Fig. 4. (a) Experimental setup of quarter-wavelength tube resonator with PVDF piezoelectric beam array. (b) output voltages and power from aligned (up) and zigzag (down) configurations with the incident sound wave of 100 dB at 146 Hz. For both configurations, the spacing between beams along the tube axis is 5 cm. Reprinted from [31], with permission from Elsevier.

Interestingly, Yang *et al* developed a broadband sound energy harvester that dual PZT piezoelectric beams located on the top of Helmholtz resonator, not located inside as shown in Fig. 5 [27]. The top wall of the Helmholtz resonator acts as a base that transforms sound energy into vibration, and the whole system can be thought as base excitation. The dual PZT piezoelectric beams with neodymium magnets placed in the middle of the top plate where the maximum acceleration applied. The resonant frequencies of the Helmholtz resonator and piezoelectric beams with magnets are matched for strong coupling effect. When the harvester is under 100 dB SPL, harvested power exhibits 0.137-1.43 mW at 170-206 Hz.

Fig. 5. (a) Schematic diagram of the proposed sound energy harvester. (b) Sound energy harvester using HR and dual piezoelectric cantilever beams. (c) Sound energy harvester using HR and single beam. (d) Conventional sound energy harvester using HR with a piezoelectric composite diaphragm. (e) Experiment setup. Reprinted from [27], with the permission of AIP Publishing.

Tapered neck Helmholtz resonator based sound energy harvester with a flexible triangular foil was introduced by Pillai *et al* as shown in Fig. 6 [37]. A polyethylene triangular foil attached to a free end of a flexible PVDF cantilever makes the cantilever in additional bending and torsion by sound pressure to increase generated power. Moreover, a tapered neck reduces the air resistance, so it also contributes to increasing power output [38]. The experiment shows that sound energy harvester using tapered neck resonator generated 673 mV at 122 Hz and 98 dB SPL, while sound energy harvester using cylindrical resonator generated just 468 mV at 125 Hz and 98 dB SPL. It is reported that input pressure should increase to observe twisting and bending simultaneously by sound energy harvester using tapered neck resonator and piezoelectric cantilever with triangular foil due to increased mass. In the experiment, the output voltage was 842 mV at 99 Hz and 103 dB SPL.

Fig. 6. Schematic of the proposed sound energy harvester. Reprinted from [37], with permission from Elsevier.

Izhar *et al* developed three degrees of freedom sound energy harvester using a Helmholtz resonator and a piezoelectric plate with a circular block and a cantilever beam as shown in Fig. 7 [39]. It was designed to broaden the narrow frequency bandwidth of conventional sound energy harvesters by adding an extra degree of freedom such as a cantilever beam. From the harvester's frequency response graph, a harvester with a cantilever beam has three resonant peaks at 1501, 1766 and 1890 Hz while harvester without a cantilever beam has two resonant peaks at 1501 and 1938 Hz. Moreover, a harvester with a cantilever beam has wider bandwidth and higher voltage output than harvester without a cantilever beam. Interestingly they used the Helmholtz resonator with a cone shape cavity instead of a conventional

Helmholtz resonator with a cylindrical cavity. It is because a Helmholtz resonator with a cone shape cavity produced higher pressure inside than a conventional Helmholtz resonator at the same incident sound pressure. According to Khan *et al*, since the Helmholtz resonator with a cone shape cavity has high acoustic stiffness compared to conventional Helmholtz resonator, resonant frequency and pressure gain increase in Helmholtz resonator with a cone shape cavity [40]. This developed sound energy harvester generated maximum power 214.23 μW under 130 dB SPL and had a bandwidth ranges from 1453-1542, 1710-1780 and 1848-1915 Hz.

Fig. 7. Three degree of freedom sound energy harvester. (a) Cross-sectional view. (b) Exploded view. Reprinted by permission from Springer Nature Terms and Conditions for RightsLink Permissions Springer Nature Customer Service Centre GmbH: Springer Nature, International Journal of Precision Engineering and Manufacturing [39], COPYRIGHT (2018).

Yuan *et al* developed a novel sound energy harvester using a helix structure as shown in Fig. 8 [41]. A helix structure tube is similar to compacted quarter-wavelength tube resonator, but there is a little difference in resonance frequency because of coupling with helix structure and a hollow disk. In addition, the helix structure can slow down wave propagation and have negative stiffness characteristics, so helix structure resonator's resonant frequency may be lower than the quarter-wavelength resonator of the same length [42,43]. They simulated the device that the total length of the helix is 412 mm, the thickness of the tube wall is 2 mm under 100 dB SPL. As a result, its fundamental resonant frequency was 193 Hz, which was the same length of 444 mm in a quarter-wavelength resonator. They used a helix sound energy harvester for low frequency sound energy harvesting. The experiment shows that the helix sound energy harvester produced 7.3 μW at the frequency of 175 Hz under 100 dB SPL.

Fig. 8. Sound energy harvester using a helix structure tube. (a) Components of proposed sound energy harvester. (b) Experimental setup. (c) Sound pressure level distribution of the sample. Reprinted from [41], with the permission of AIP Publishing.

Same researcher group as above, Yuan *et al* developed a sound energy harvester based on a

spiral Helmholtz resonator as shown in Fig. 9 [25]. They chose a spiral structure because of its low resonant frequency characteristic that curved neck inlet and outlet could reduce the acoustic resonant frequency [44]. The experiments compared the cavity with a tapered neck and non-tapered neck, sound energy harvester with a proof mass and without a proof mass. The first experiment result shows that the cavity with a tapered neck has a higher resonant frequency and higher pressure amplification ability. It is because the tapered neck that varies the cross-sectional area smoothly can reduce viscous loss [37]. Another experiment result shows that the sound energy harvester with a proof mass has 27.2 μW at acoustic resonance 217 Hz, 64.4 μW at mechanical resonance 341 Hz while the sound energy harvester without a proof mass 12.1 μW at acoustic resonance 221 Hz (almost same), 13.4 μW at mechanical resonance 611 Hz. It means that proof mass has little effect on acoustic resonance, while it affects mechanical resonance significantly. Furthermore, proof mass increases the maximum harvested power, especially at mechanical resonance.

Fig. 9. (a) Sound energy harvester based on a spiral Helmholtz resonator. (b) Components of the proposed sound energy harvester. (c) Photograph of experimental setup. Reprinted from [25] under a CC BY license.

Electromagnetic sound energy harvesters are based on Faraday's law of electromagnetic induction that the rate at which magnetic flux through the loop changes with time induced the electromotive force in a closed loop [45]. A typical electromagnetic sound energy harvester has a resonator, membrane same as a piezoelectric sound energy harvester. However, a fixed coil and a magnet attached to the membrane are used for electromagnetic induction as shown in Fig. 10.

Fig. 10. Schematic of electromagnetic sound energy harvester.

When the amplified sound wave by a resonator makes the membrane vibrates, a magnet attached to the membrane also vibrates so related movement between the magnet and coil occurs. It causes the magnetic flux change, so an electromotive force is generated through the coil. In case of Khan *et al*, which has an almost similar structure to Fig. 10, maximum voltage

and power output were 319.8 mV and 1.96 mW at 143 Hz under 125 dB SPL [46].

Lai *et al* developed the micro-scale electromagnetic sound energy harvester for portable electronics [47]. It contains a nickel planar coil and a neodymium magnet attached to the suspension plate. The planar coil and suspension plate are fabricated on a 500 μm thick, double-sided thermally oxidized silicon wafer by thermal evaporation, photolithography, electro-deposition, and wet etching process. The device has the 3 mm × 3 mm × 1 mm size, and harvested power is 0.24 mV open circuit voltage at the resonant frequency of 470 Hz when the distance between the 3 W power speaker and micro-scale sound energy harvester is 5 mm.

Izhar *et al* developed the electromagnetic sound energy harvester with a cone-shaped Helmholtz cavity [48]. As previously mentioned in three degrees of freedom piezoelectric sound energy harvester [39,40], a cone-shaped cavity has a higher stiffness than the cylindrical cavity, so it contributes to increasing resonant frequency and pressure amplification. The developed sound energy harvester has two wound coils to maximize power output that one is a cylindrical type surrounded by the magnet, and another is a circular disc type under the magnet. In the experiment, there are two resonant peaks of 330.3 Hz and 1332 Hz that lower one refers to a membrane with a magnet, a higher one refers to Helmholtz resonator. Air gaps are added in the coil holder to reduce the air damping loss. The device harvested the total maximum power of 212 μW at 330.3 Hz and 100 dB SPL.

Among resonator based sound energy harvesters, using triboelectric effect, which is a type of contact electrification, is not common. Yang *et al* first developed the triboelectric sound energy harvester by utilizing a Helmholtz resonator as shown in Fig. 11 [49]. In case of [49], the only membrane changed to separated multi-layer from the typical sound energy harvester. Separated multi-layer is composed of an aluminum thin film with nanopores and a layer of polytetrafluoroethylene (PTFE) film with deposited copper. The aluminum thin film serves as both a contact surface and an electrode, PTFE film acts as another electrode. When a sound wave is incident, resonator amplifies the incident sound pressure, and PTFE film will vibrate and repeat the cycle of contacting and separation. Therefore, electricity is generated every cycle of contacting and separation. This device generated a maximum electric power density of 60.2 $mW \cdot m^{-2}$, which corresponds to the power of about 376 μW at 110 dB SPL. Furthermore, it can be used for distance measurement sensor and an active sensor for sound source localization. So it can be used for a self-powered acoustic sensor.

Fig. 11. Structural design of the organic film nanogenerators. (a) Sketch and (b) cross-sectional view of the nanogenerator. (c) SEM image of nanopores on aluminum electrode. (d) SEM image of PTFE nanowires fabricated on the film surface by plasma etching, which largely increase the triboelectrification. Reprinted with permission from [49]. Copyright (2014) American Chemical Society.

2.3 Acoustic metamaterial based sound energy harvesters

Acoustic metamaterials are a kind of composite systems that are designed to control, direct, and manipulate sound waves at certain frequencies in ways that are not observed in nature [50,51]. Acoustic metamaterials can control sound waves by creating an artificial periodic geometry using conventional materials such as metal and plastic. Acoustic metamaterial based sound energy harvesters use the local resonance that sound wave localizes inside the metamaterial as shown in Fig 12(a). It is possible to decrease the size of whole harvesting devices for low frequency energy harvesting because the local resonant frequency of metamaterials usually depends on the geometrical arrangement and the material properties, rather than the dimension of the structure [52,53]. There are two types of acoustic metamaterials introduced in here, which are phononic crystal and sonic crystal. Phononic crystal is a periodic artificial structure made of sonic scatterers embedded in a host material that is similar to scatterer material, such as copper cylinders embedded in an aluminum matrix. However, sonic crystal, which was first proposed by Liu *et al* [54], is composed of periodic arrangements of sonic scatterers embedded in a host material with different mechanical properties such as solid structures allocated in the fluid. Phononic crystal with a solid host material is usually for elastic wave propagation including both longitudinal and transverse wave. For example, Carrara *et al* proposed several concepts of elastoacoustic wave energy harvesters by using a phononic crystal that consists of aluminum cylindrical stubs embedded in aluminum plate, such as a parabolic acoustic mirror, point defect, and acoustic funnel [55]. In contrast, a sonic crystal is considered to be only dependent on the longitudinal wave component [56,57]. Phononic crystal and sonic crystal have the bandgaps that can block the propagating elastic waves at specific frequencies so the wave energy can be localized in the structure at the frequency of the defect band [58]. The defect band is generated by breaking the symmetry of the metamaterial and acts as a narrow frequency pass

band between the bandgap. From Fig. 12(b), a sound transmission loss of the acoustic metamaterial is almost zero at the defect mode. That is, high sound transmission is observed at the defect mode. For sound energy harvesting, energy conversion device should be located in energy localized zone, and it can convert sound energy into electrical energy.

Fig. 12. (a) Pressure distribution of the acoustic metamaterial at the defect mode. (b) Sound transmission loss of the acoustic metamaterial versus sonic frequency.

Wu *et al* designed the sound energy harvester that consists of piezoelectric PVDF film and two dimensional 5×5 sonic crystal made of 40 cm length, 3.5 cm diameter polymethyl methacrylate (PMMA) cylinders with square array embedded in air background [59]. A point defect occurs in the middle of the crystal by removing one cylinder in the middle, and it acts as a resonant cavity at a resonant frequency. PVDF film is placed in the cavity of sonic crystal and converts localized sound energy into electrical energy as much as possible. At the frequency of 4.2 kHz, the largest pressure is observed in the middle of the cavity. Moreover, the output voltage with the sonic crystal is 25 times bigger than that without the sonic crystal at 4.2 kHz. The maximum power was about 40 nW at the resonant frequency of 4.2 kHz.

In the further study at the same research group, Wang *et al* presented the modeling of sound energy harvester with a piezoelectric curved beam in the cavity of sonic crystal and showed some simulation results and experimental results [60]. From the simulation results of pressure distribution and the particle velocity field in a sonic crystal, center of the resonant cavity has the highest pressure and relatively low particle velocity, while surrounding area of the resonant cavity has the lowest pressure and highest particle velocity. Therefore, the pressure difference between two sides of the curved beam can be maximized around the center of the cavity. The pressure difference between two sides of the beam, which is the source to oscillate the piezoelectric curved beam, is measured about 7 Pa, same as 110.88 dB SPL in the experiment. The maximum power was generated approximately 37 nW at 4.21 kHz.

Qi *et al* developed a sound energy harvester based on a planar acoustic metamaterial [61]. Phononic crystal is composed of a periodic array of 6×6 silicone rubber cylinders embedded in a 6 cm square thin homogeneous aluminum plate that is located in the x-y plane. By removing four cylinders in the center, a point defect is generated and strain energy originated

from the z-axis sound wave is concentrated in the center. Therefore, the PZT patch is attached to the defected center region to maximize harvested energy. The maximum output voltage and power are measured as 1.3 V and 8.8 μW at 2257.5 Hz and incident sound pressure of 2 Pa, which is same as 100 dB in sound pressure level.

Sun *et al* developed the sound energy harvester using a doubly coiled-up acoustic metamaterial cavity to harvest the low frequency sound wave [44]. It is known that this double-walled acoustic metamaterial cavity with a small gap can enhance the sound emission and sound pressure because of the Fabry-Perot resonance [62,63]. Moreover, an acoustic metamaterial cavity can be made by periodic zigzag elements at the subwavelength-scale because of the high refractive index that is achieved by zigzag space [64]. Piezoelectric PZT bimorph plate with a brass tip mass is located in the cavity and convert the sound energy into electric energy. Voltage gain, which means the ratio of the output voltage with and without cavity, is about 16 dB. In other words, the incident sound pressure level will be increased up to 16 dB. In the experiment, the optimal cavity gap is 30 mm in this case, when the gap is closer or further, the output voltage decreases. It is because of resonance matching between the cavity and PZT plate. The maximum output voltage and power are measured as 258.5 mV and 0.345 μW at 600 Hz and incident SPL of 100 dB.

The quarter-wavelength resonator phononic crystal can be used to collect sound energy by sound localization effect. It consists of several quarter-wavelength resonators, a wave duct, and piezoelectric vibrators and it has several band gaps that transmission ratio is almost zero. Guo *et al* developed the sound energy harvester based on a quarter-wavelength resonator phononic crystal as shown in Fig. 13 [65]. When the sound wave is incident to the inlet of the main duct, piezoelectric vibrators that replaced the closed ends of the quarter-wavelength resonators oscillate and convert sound energy into electrical energy. From the experiment results, the maximum output voltage occurs at the boundaries of the bandgaps since the acoustic impedance rapidly decreases at the inlet of resonators. In other words, the strong coupling interaction between each resonator enhances the local resonance. Moreover, it shows that piezoelectric vibrator in the middle of the main duct generates more voltage output than other piezoelectric vibrators. The maximum output voltage is about 17 mV at the fourth quarter-wavelength resonators of total seven resonators from the duct inlet exciting as 710 Hz under an incident sound pressure of 1.0 Pa, which is same as sound pressure level of 94 dB. It is reported that resistance of 5100 Ω is used, so the maximum harvested power is

estimated about 56.67 nW.

Fig. 13. Schematic of the sound energy harvesting system (a) Quarter-wavelength resonator phononic crystal (b) Piezoelectric vibrators (c) Block diagram and experimental setup. Reprinted from [65] under a CC BY license.

Yuan *et al* developed the acoustic metastructure based sound energy harvester for low frequency sound isolation and sound energy harvesting [66]. Acoustic metastructure consists of a metallic substrate, PZT piezoelectric patch, and proof mass as shown in Fig. 14. Because of using a metallic substrate instead of elastic rubber film, membrane tension process before adding mass to the membrane is not needed, and durability is enhanced [67]. From the simulation results, the structure's effective dynamic mass density is zero around the first resonant frequency due to structural damping, and it increases gradually and drops sharply into a negative region with increasing frequency. The negative dynamic mass property leads the transmitted sound decrease exponentially [68]. The larger effective mass density, the smaller displacement occurs and causes big sound transmission loss. In the experiment, there is a geometrical effect of the proof mass about energy harvesting performance. For the same proof mass weight, proof mass with larger area generates smaller power because the bonding surface covered by the proof mass does not generate strain. The harvested power is 0.21 mW at 155 Hz and incident 114 dB SPL, which is the same value as 10 Pa.

Fig. 14. (a) Schematic diagram of the metamaterial structure. (b) Experimental setup. Reprinted from [66] under a CC BY license.

Javadi *et al* designed a 1D sonic array based triboelectric sound energy harvester with carbon nanotubes (CNTs) as shown in Fig. 15(a) [69]. The triboelectric sound energy harvester consists of top electrode with a 500 μm thickness steel, a middle spacer with a 25 μm thickness Kapton tape, and a bottom electrode with a 40 μm thickness steel coated by a layer of polydimethylsiloxane (PDMS) with a thickness of 10 μm. There are acoustic holes with a diameter of 200 μm and a spacing distance of 1 cm in the top steel plate. Therefore, an incident sound wave can transfer the dynamic pressure to PDMS/steel composite plate. CNTs

are spread on the top electrode to enhance the harvested power by increasing the effective contact area. Due to its high electrical conductivity, good mechanical, electrical properties, flexibility, robustness, and high surface area, it is widely used in triboelectric energy harvesting [70-74]. When the sound wave is incident to the top steel plate, the bottom composite plate oscillates, and the bottom PDMS layer repeats the contact and separation with a top steel plate. Triboelectric charges are produced at the contacting surfaces, each positive and negative charges are generated on the top steel electrode and the bottom PDMS layer. Since the charge moves, the output current is observed in the external circuit, and output power is generated when the external impedance exists. In the experiment, triboelectric sound energy harvester has an output open circuit voltage about 40 mV (with CNTs) and 25 mV (without CNTs) under input sound power around 10 W. By using this triboelectric sound energy harvester and four steel slabs with a 500 μm thickness, 1D sonic crystal array is constructed to use local resonance effect. According to Fig. 15(b), sound pressure difference is maximized in the middle steel slab, so the triboelectric sound energy harvester replaces the middle steel plate to achieve the higher output power. The measured output power is about 40 nW at a resonant frequency of 4.24 kHz and an external load of 1 MΩ under the incident sound power of about 10^{-7} W. Moreover, the output power of triboelectric energy harvester embedded inside the sonic array is higher than free triboelectric energy harvester at the resonant frequency of 4.24 kHz, while the output power of triboelectric energy harvester embedded inside the sonic array is lower at the off-resonance frequency of 6.5 kHz.

Fig. 15. Schematic of the proposed sound energy harvester. (a) Triboelectric sound energy harvester with CNTs. (b) 1D sonic crystal array configuration and sound pressure distribution. Reprinted from [69], with permission from Elsevier.

2.4 Other kinds of sound energy harvesters

This paragraph introduces another three different types of sound energy harvesters. The first type is about using a hybrid method. Yang *et al* made a hybrid of pressure amplification methods by using both sonic crystal with a resonant cavity and an electromechanical Helmholtz resonator (EMHR) [75]. Sonic crystal resonator (SCR) consists of 5×5

polymethyl methacrylate (PMMA) cylinders that the center of the sonic crystal is removed and it is embedded in air background as shown in Fig. 16. SCR structure has the same resonant frequency as EMHR structure with a piezoelectric composite diaphragm to increase energy harvesting performance by coupled resonance structure. In the experiment, the acoustic pressure gains of the SCR structure and EMHR structure are 5.5 and 5.0 at 5.535 kHz respectively, while the coupled resonance structure is 28.0 at 5.545 kHz. It shows that a strong acoustic resonance coupling between the sonic crystal resonator and the Helmholtz resonator occurs, so the large pressure amplification and little frequency change is observed. The maximum harvested power and the corresponding peak-to-peak voltage are 429 μW and 3.89 V at the resonant frequency of 5.545 kHz with 110 dB SPL.

Fig. 16. (a) Structure diagram of the SCR structure. (b) Structure diagram of the EMHR structure. (c) Structure diagram of the coupled resonance structure. (d) Photograph of the proposed harvester with the coupled resonance structure. Copyright 2013 The Japan Society of Applied Physics.

In the further study, Yang *et al* made a similar sound energy harvester that uses both Helmholtz resonator (EMHR) and cross-plate phononic crystal resonator (Cr-PCR) with a defect by removing a cross plate as shown in Fig. 17 [76]. Phononic crystal resonator consists of 3×3 copper cross plates with a defect in the middle. The simulation result of pressure amplification shows that when plate thickness is far less than a width of the cross plate, high pressure amplification, which is the same meaning as high Q-value occurs. It is because of the strong directional wave-scattering effect of the cross-plate corners, and strong localization effect is observed. The maximum output power and corresponding voltage output are measured as 578 μW and 4.3 V at a resonant frequency of 6.975 kHz under 100 dB SPL. These results show the higher harvesting performance of cross-plate resonator than the previous study.

Fig. 17. (a) Structure diagram of the high-Q Cr-PCR structure. (b) Structure diagram of the EMHR structure. (c) Structure diagram of the coupled resonance structure. (d) Photograph of the proposed harvester with the coupled resonance structure. Copyright 2015 The Japan

Society of Applied Physics.

There is another way to use a hybrid method besides the hybrid of pressure amplification method. Khan *et al* designed the sound energy harvester that uses a hybrid of energy conversion method [77]. The harvester is composed of Helmholtz resonator, piezoelectric plate with magnets, and wound circular coil. As you can guess, it uses both piezoelectric and electromagnetic energy conversion methods to harvest sound energy as much as possible. The measured output voltage and maximum power are 223 mV and 50 μW at an optimal load of 1000 Ω and 2100 Hz resonant frequency with 130 dB SPL from the piezoelectric portion, 38 mV and 2.86 μW at an optimal load of 114 Ω and 2100 Hz resonant frequency with 130 dB SPL from the electromagnetic portion.

The second type of another sound energy harvester is that using only triboelectric nanogenerator (TENG) without pressure amplification things such as a resonator. The triboelectric nanogenerator is based on the principle of coupling between contact electrification and electrostatic induction, and it converts mechanical energy into electric energy [78,79]. Cui *et al* developed a triboelectric sound energy harvester with two substrates and one vibrating membrane as shown in Fig. 18 [80]. A top substrate with a stainless steel mesh and PVDF nanofibers is a top electrode, and bottom substrate with an aluminum mesh is the contact surface and bottom electrode. The mesh structure is selected because of the air circulation and benefits to the propagation of the sound wave. Vibrating membrane is composed of two spacers and polyethylene film coated with PVDF nanofibers and aluminum thin film at each side. Due to incident sound wave, vibrating membrane oscillates and repeats contact and separation between aluminum and PVDF nanofibers so the current flows. The maximum short-circuit current and the output voltage of 0.01 m^2 TENG are measured as 0.45 mA and 70 V at 160 Hz and 114 dB SPL, 0.18 mA and 90 V at 175 Hz and 100 dB SPL. Moreover, the proposed sound energy harvester has a charging rate of 61 μC/s and a maximum power density of 202 mW/m^2. The durability of this harvester is verified that there is no degradation of device's current output for 7 days.

Fig. 18. (a) Schematic of a fabricated sound driven TENG. (b) SEM image of the PVDF nanofibers on the stainless steel mesh. (c) Working mechanism of the sound driven TENG. (d)

The output current signal in one cycle. Reprinted from [80], with permission from Elsevier.

The same researcher group, Liu *et al* made an integrated triboelectric nanogenerator (ITNG) with a three-dimensional structure to improve the ability of harvesting sound energy without a resonator [81]. The sound driven ITNG has repeated arrangement of layer A and B. Layer A consists of polyvinylidene fluoride (PVDF) nanofibers, spacer and aluminum coated porous polyvinyl chloride (PVC) substrate between the PVDF nanofibers and spacer. Layer B is composed of PVDF nanofibers, polyethylene (PE) substrate, an aluminum layer, and spacer. Layer A is the basic structure, and layer B acts as the vibrating membrane. The pore array of the PVC substrate with an average diameter of 1 mm makes the air circulation and sound propagation possible, which leads to transfer more sound energy to vibration membrane. Aluminum layer acts as both a friction layer and an electrode. When the sound wave is incident to ITNG, the sound wave propagates and makes the vibrating membrane layer B oscillates. Then, PVDF nanofibers of layer B repeat contact and separation with an aluminum layer of bottom layer A, while an aluminum layer of layer B repeats separation and contact with PVDF nanofibers of top layer A. There is no charge generation at origin state, but the charge is generated after a certain time of vibration. Positive charge flow from layer B to layer A is observed when the contact with the bottom layer A and layer B or the separation with the top layer A and layer B occurs. On the other hand, positive charge flow from layer A to layer B is observed when the separation with the bottom layer A and layer B or the contact with the top layer A and layer B occurs. The maximum short-circuit current of 9.5 cm × 9.5 cm ITNG is measured as 2.1 mA when the number of working units is four at 200 Hz and 100.5 dB SPL, and the maximum open-circuit voltage 232 V when the number of working units is one at 200 Hz and 100.5 dB SPL, which are 4.6 times and 2.6 times as large as the previous study. In addition, the proposed sound energy harvester has a maximum power density of 5414.9 mW/m^2 and a maximum charging rate of 453 μC/s for a 1 mF capacitor, which are 26.8 times and 7.4 times the highest values than the previous study.

The last type is unique that sound energy harvester with multi-stable characteristics. Zhou *et al* developed a bi-stable sound energy harvester for harvesting broadband noise energy [82]. The bi-stable sound energy harvester consists of a piezoelectric beam with a flat plate, a curved plate, a movable magnet and a fixed magnet as shown in Fig. 19. The fixed magnet has the same polarity as the movable magnet to apply repulsive force for stability. The bi-

stable sound energy harvester's aim is transferring the high frequency vibration to the low frequency response, which the harvester can create a quite large amplitude's response and generate a high output voltage and power. It is good for harvesting a wide range of frequency such as noise. From the simulation and experiment results, the system has two stable equilibrium positions and can jump between them in a noisy environment by adjusting the separation distance between the tip magnet and the fixed magnet. In other words, the bi-stable sound energy harvester can realize snap-through between equilibrium positions and maintain coherence resonance under broadband noise and thus generate high output power. Moreover, the separation distance can be optimized according to a given SPL to lead coherence resonance and generate the largest output power. For reference, open-circuit RMS voltage has a maximum value of 0.4 V at incident SPL of 105 dB and the separation distance of 17 mm, while the variance of strain has a maximum value of 1.1×10^{-8} at incident SPL of 105 dB and the separation distance of 16.8 mm.

Fig. 19. (a) Schematic of the bi-stable sound energy harvester. (b) Experimental setups. Reprinted from [82], with permission from Elsevier.

3. Summary and conclusion

Summaries of sound energy harvesters introduced in this paper are presented in the following pages. Brief details of resonator based sound energy harvesters are listed in Table 2, acoustic metamaterial based sound energy harvesters are listed in Table 3, and other kinds of sound energy harvesters are listed in Table 4.

Table 2. Summary of resonator based sound energy harvesters.

Table 3. Summary of acoustic metamaterial based sound energy harvesters.

Table 4. Summary of other kinds of sound energy harvesters.

The comparison criteria of the introduced sound energy harvesters are energy conversion

type, device size, incident sound pressure level, harvester's load impedance, resonant frequency or operation frequency, voltage output, and generated power. From the perspective of energy conversion type, generally electromagnetic sound energy harvesters have lower load impedance than piezoelectric type and triboelectric type. In case of triboelectric sound energy harvesters in Table 4 (using only triboelectric sound energy harvester), the load resistance is comparable to electromagnetic type, so it contributes to large harvested power. Furthermore, triboelectric sound energy harvesters tend to deteriorate harvesting performance when the pressure amplification methods are applied together. Compared to acoustic metamaterial based sound energy harvesters, resonator based sound energy harvesters generate more output power. It means that resonator is more effective to amplify pressure than acoustic metamaterial over a certain sound pressure level. Acoustic metamaterial based sound energy harvesters have been studied a lot in recent years because of their useful characteristic that not depends on device's dimension. Therefore, acoustic metamaterial based sound energy harvesters are more applicable at low SPL, low frequency, and subwavelength scale than resonator based sound energy harvesters. The reported sound energy harvester's sizes and powers are in the range of 0.009 – 9236.28 cm^3 and 6×10^{-6} – 48.87×10^3 μW. This paper shows the comprehensive simple review about the sound energy harvesting. There are various approaches about transduction mechanism, incident pressure amplification methods to harvest electrical energy from ambient sound energy.

Unfortunately, like other energy harvesters, sound energy harvesters are still less used in real situations including WSNs. One of the critical issues is unstable system conditions such as varying incident frequency and sound pressure level that changed by some unexpected variables. From the perspective for future research and applications, sound energy harvesters should be able to respond to surrounding environment changes. There are several efforts to overcome this problem introduced in this paper such as wide-bandwidth sound energy harvesters by increasing degrees of freedom and nonlinear multi-stable sound energy harvesters. However, it is just in the early stages, so it is needed to research various methods. Another issue is the low sound pressure level of the usual sound source. From table 2, 3, and 4, almost the whole sound energy harvesters are characterized at above 100 dB SPL which is greater than or equal to noise generated by jack hammer or basic metal industry. It is relatively higher SPL than ordinary SPL such as normal conversation (40 - 60 dB). Therefore, it is necessary to research for universal use that generates sufficient power even at low SPL.

In recent months, there are several studies to apply sound energy harvesters in real high-speed railways [83,84]. Likewise, it is important to install and test sound energy harvesters in real situations. Therefore, it is necessary to measure real environment system conditions to design sound energy harvesters properly for real-life applications. It is expected that after overcoming several limitations, sound energy harvesters will be widely used in the near future.

Acknowledgment

This work was supported by the Energy Technology Development Project (KETEP) grant funded by the Ministry of Trade, Industry and Energy, Republic of Korea (Development of energy harvesting materials and modules for autonomous power of smart sensors, Project no. 20182010106361), the Institutional Research Program of the Korea Institute of Science and Technology (2E28210), the National Research Council of Science & Technology (NST) grant by the Korea government (MSIP) (No. CAP-17-04-KRISS) and KU-KIST Research Program of Korea University (R1309521).

References

[1] P.P. Ray, A survey on Internet of Things architectures, J. King Saud Univ. - Comput. Inf. Sci. 30 (2018) 291–319. doi:10.1016/j.jksuci.2016.10.003.
[2] J. Gubbi, R. Buyya, S. Marusic, M. Palaniswami, Internet of Things (IoT): A vision, architectural elements, and future directions, Futur. Gener. Comput. Syst. 29 (2013) 1645–1660. doi:10.1016/j.future.2013.01.010.
[3] M. Díaz, C. Martín, B. Rubio, State-of-the-art, challenges, and open issues in the integration of Internet of things and cloud computing, J. Netw. Comput. Appl. 67 (2016) 99–117. doi:10.1016/j.jnca.2016.01.010.
[4] M. Ramakrishnan, G. Rajan, Y. Semenova, G. Farrell, Overview of Fiber Optic Sensor Technologies for Strain/Temperature Sensing Applications in Composite Materials, Sensors. 16 (2016) 99. doi:10.3390/s16010099.
[5] A. Servent, S. Daskalakis, A. Collado, A. Georgiadis, A proximity wireless sensor based on backscatter communication, 2017 Int. Appl. Comput. Electromagn. Soc. Symp. - Italy, ACES 2017. (2017) 1–2. doi:10.23919/ROPACES.2017.7916349.
[6] S.E. Li, G. Li, J. Yu, C. Liu, B. Cheng, J. Wang, K. Li, Kalman filter-based tracking of moving objects using linear ultrasonic sensor array for road vehicles, Mech. Syst. Signal Process. 98 (2018) 173–189. doi:10.1016/j.ymssp.2017.04.041.
[7] N. Yamazoe, Toward innovations of gas sensor technology, Sensors Actuators, B Chem. 108 (2005) 2–14. doi:10.1016/j.snb.2004.12.075.

[8] Y.G. Song, Y.S. Shim, S. Kim, S.D. Han, H.G. Moon, M.S. Noh, K. Lee, H.R. Lee, J.S. Kim, B.K. Ju, C.Y. Kang, Downsizing gas sensors based on semiconducting metal oxide: Effects of electrodes on gas sensing properties, Sensors Actuators, B Chem. 248 (2017) 949–956. doi:10.1016/j.snb.2017.02.035.
[9] G. Zhou, L. Huang, W. Li, Z. Zhu, Harvesting ambient environmental energy for wireless sensor networks: A survey, J. Sensors. 2014 (2014). doi:10.1155/2014/815467.
[10] C. Abreu, P. Mendes, Wireless Sensor Networks for Biomedical Applications, Bioeng. (ENBENG), 2013 IEEE 3rd Port. Meet. (2013) 1–4. doi: 10.1109/ENBENG.2013.6518413.
[11] M. reza Akhondi, A. Talevski, S. Carlsen, S. Petersen, Applications of Wireless Sensor Networks in the Oil, Gas and Resources Industries, 2010 24th IEEE Int. Conf. Adv. Inf. Netw. Appl. (2010) 941–948. doi:10.1109/AINA.2010.18.
[12] M.Z.A. Bhuiyan, G. Wang, J. Wu, J. Cao, X. Liu, T. Wang, Dependable Structural Health Monitoring Using Wireless Sensor Networks, Ieee Trans. Dependable Secur. Comput. 14 (2012) 363–376. doi: 10.1109/TDSC.2015.2469655.
[13] S.D.T. Kelly, N.K. Suryadevara, S.C. Mukhopadhyay, Towards the implementation of IoT for environmental condition monitoring in homes, IEEE Sens. J. 13 (2013) 3846–3853. doi:10.1109/JSEN.2013.2263379.
[14] F.T. Jaigirdar, M.M. Islam, S.R. Huq, An efficient and cost effective maximum clique analysis based approximation in military application of wireless sensor network, 14th Int. Conf. Comput. Inf. Technol. ICCIT 2011. (2011) 85–90. doi:10.1109/ICCITechn.2011.6164879.
[15] M.P. Durisic, Z. Tafa, G. Dimic, V. Milutinovic, A survey of military applications of wireless sensor networks, Mediterr. Conf. Embed. Comput. 2012. (2012) 196–199.
[16] K.A. Cook-Chennault, N. Thambi, A.M. Sastry, Powering MEMS portable devices - A review of non-regenerative and regenerative power supply systems with special emphasis on piezoelectric energy harvesting systems, Smart Mater. Struct. 17 (2008). doi:10.1088/0964-1726/17/4/043001.
[17] I. Jung, Y.H. Shin, S. Kim, J. young Choi, C.Y. Kang, Flexible piezoelectric polymer-based energy harvesting system for roadway applications, Appl. Energy. 197 (2017) 222–229. doi:10.1016/j.apenergy.2017.04.020.
[18] Y.H. Shin, I. Jung, M.S. Noh, J.H. Kim, J.Y. Choi, S. Kim, C.Y. Kang, Piezoelectric polymer-based roadway energy harvesting via displacement amplification module, Appl. Energy. 216 (2018) 741–750. doi:10.1016/j.apenergy.2018.02.074.
[19] W.J.G. Ferguson, Y. Kuang, K.E. Evans, C.W. Smith, M. Zhu, Auxetic structure for increased power output of strain vibration energy harvester, Sensors Actuators A Phys. 282 (2018) 90–96. doi:10.1016/j.sna.2018.09.019.
[20] A. Cuadras, M. Gasulla, V. Ferrari, Thermal energy harvesting through pyroelectricity, Sensors Actuators, A Phys. 158 (2010) 132–139. doi:10.1016/j.sna.2009.12.018.
[21] S. Orrego, K. Shoele, A. Ruas, K. Doran, B. Caggiano, R. Mittal, S.H. Kang, Harvesting ambient wind energy with an inverted piezoelectric flag, Appl. Energy. 194 (2017) 212–222. doi:10.1016/j.apenergy.2017.03.016.
[22] J. Sarwar, G. Georgakis, K. Kouloulias, K.E. Kakosimos, Experimental and numerical investigation of the aperture size effect on the efficient solar energy harvesting for solar

thermochemical applications, Energy Convers. Manag. 92 (2015) 331–341. doi:10.1016/j.enconman.2014.12.065.
[23] S.Y. Chang, P. Cheng, G. Li, Y. Yang, Transparent Polymer Photovoltaics for Solar Energy Harvesting and Beyond, Joule. 2 (2018) 1039–1054. doi:10.1016/j.joule.2018.04.005.
[24] M. Yuan, H. Ji, J. Qiu, T. Ma, Active control of sound transmission through a stiffened panel using a hybrid control strategy, J. Intell. Mater. Syst. Struct. 23 (2012) 791–803. doi:10.1177/1045389X12439638.
[25] M. Yuan, Z. Cao, J. Luo, Z. Pang, Low frequency acoustic energy harvester based on a planar Helmholtz resonator, AIP Adv. 085012 (2018). doi:10.1063/1.5042683.
[26] Wikipedia, Sound pressure. https://en.wikipedia.org/wiki/Sound_pressure, 2018 (accessed 8 September 2018).
[27] A. Yang, P. Li, Y. Wen, C. Lu, X. Peng, W. He, J. Zhang, D. Wang, F. Yang, Note: High-efficiency broadband acoustic energy harvesting using Helmholtz resonator and dual piezoelectric cantilever beams, Rev. Sci. Instrum. 85 (2014) 1–4. doi:10.1063/1.4882316.
[28] F. Liu, A. Phipps, S. Horowitz, K. Ngo, L. Cattafesta, T. Nishida, M. Sheplak, Acoustic energy harvesting using an electromechanical Helmholtz resonator, J. Acoust. Soc. Am. 123 (2008) 1983–1990. doi:10.1121/1.2839000.
[29] M. Yuan, Z. Cao, J. Luo, J. Zhang, C. Chang, An efficient low-frequency acoustic energy harvester, Sensors Actuators, A Phys. 264 (2017) 84–89. doi:10.1016/j.sna.2017.07.051.
[30] B. Li, J.H. You, Y.J. Kim, Low frequency acoustic energy harvesting using PZT piezoelectric plates in a straight tube resonator, Smart Mater. Struct. 22 (2013). doi:10.1088/0964-1726/22/5/055013.
[31] B. Li, A.J. Laviage, J.H. You, Y.J. Kim, Harvesting low-frequency acoustic energy using multiple PVDF beam arrays in quarter-wavelength acoustic resonator, Appl. Acoust. 74 (2013) 1271–1278. doi:10.1016/j.apacoust.2013.04.015.
[32] D. T. Blackstock, Fundamentals of Physical Acoustics, John Wiley & Sons, New York, 2000.
[33] M. Alster, Improved calculation of resonant frequencies of Helmholtz resonators, J. Sound Vib. 24 (1972) 63–85. doi:10.1016/0022-460X(72)90123-X.
[34] C.H. Sohn, J.H. Park, A comparative study on acoustic damping induced by half-wave, quarter-wave, and Helmholtz resonators, Aerosp. Sci. Technol. 15 (2011) 606–614. doi:10.1016/j.ast.2010.12.004.
[35] S.B. Horowitz, M. Sheplak, L.N. Cattafesta, T. Nishida, A MEMS acoustic energy harvester, J. Micromechanics Microengineering. 16 (2006) 13–16. doi:10.1088/0960-1317/16/9/S02.
[36] B. Li, J.H. You, Simulation of Acoustic Energy Harvesting Using Piezoelectric Plates in a Quarter-wavelength Straight-tube Resonator, Proc. 2012 COMSOL Conf. Bost. (2012).
[37] M.A. Pillai, D. Ezhilarasi, Improved Acoustic Energy Harvester Using Tapered Neck Helmholtz Resonator and Piezoelectric Cantilever Undergoing Concurrent Bending and Twisting, Procedia Eng. 144 (2016) 674–681. doi:10.1016/j.proeng.2016.05.065.
[38] S.K. Tang, On Helmholtz resonators with tapered necks, J. Sound Vib. 279 (2005) 1085–1096. doi:10.1016/j.jsv.2003.11.032.
[39] Izhar, F.U. Khan, Three degree of freedom acoustic energy harvester using improved

Helmholtz resonator, Int. J. Precis. Eng. Manuf. 19 (2018) 143–154. doi:10.1007/s12541-018-0017-z.
[40] F.U. Khan, An Improved Design of Helmholtz Resonator for Acoustic Energy Harvesting Devices, Rev. Sci. Instrum. (2016) 2–7. doi:10.1109/INTELSE.2016.7475135.
[41] M. Yuan, Z. Cao, J. Luo, Z. Pang, Helix structure for low frequency acoustic energy harvesting, Rev. Sci. Instrum. 89 (2018). doi:10.1063/1.5021526.
[42] X. Zhu, K. Li, P. Zhang, J. Zhu, J. Zhang, C. Tian, S. Liu, Implementation of dispersion-free slow acoustic wave propagation and phase engineering with helical-structured metamaterials, Nat. Commun. 7 (2016) 1–7. doi:10.1038/ncomms11731.
[43] F. Ma, J.H. Wu, M. Huang, G. Fu, C. Bai, Cochlear bionic acoustic metamaterials, Appl. Phys. Lett. 105 (2014). doi:10.1063/1.4902869.
[44] K.H. Sun, J.E. Kim, J. Kim, K. Song, Sound energy harvesting using a doubly coiled-up acoustic metamaterial cavity, Smart Mater. Struct. 26 (2017). doi:10.1088/1361-665X/aa724e.
[45] J. Walker, D. Halliday, R. Resnick, Fundamentals of Physics, tenth ed., John Wiley & Sons, New York, 2015.
[46] F.U. Khan, Izhar, Electromagnetic-based acoustic energy harvester, Proc. 16th Int. Multi Top. Conf. INMIC 2013. (2013) 125–130. doi:10.1109/INMIC.2013.6731337.
[47] T. Lai, C. Huang, C. Tsou, Design and fabrication of acoustic wave actuated microgenerator for portable electronic devices, DTIP MEMS MOEMS - Symp. Des. Test, Integr. Packag. MEMS/MOEMS. (2008) 28–33. doi:10.1109/DTIP.2008.4752946.
[48] Izhar, F.U. Khan, Electromagnetic based acoustic energy harvester for low power wireless autonomous sensor applications, Sens. Rev. 38 (2018) 298–310. doi:10.1108/SR-04-2017-0062.
[49] J. Yang, J. Chen, Y. Liu, W. Yang, Y. Su, Z.L. Wang, Triboelectrification-based organic film nanogenerator for acoustic energy harvesting and self-powered active acoustic sensing, ACS Nano. 8 (2014) 2649–2657. doi:10.1021/nn4063616.
[50] S.A. Cummer, J. Christensen, A. Alù, Controlling sound with acoustic metamaterials, Nat. Rev. Mater. (2016). doi:10.1038/natrevmats.2016.1.
[51] APS physics, Synopsis: Sound Switch. https://physics.aps.org/synopsis-for/10.1103/PhysRevLett.113.014301, 2018 (accessed 8 September 2018).
[52] N. Aravantinos-Zafiris, M.M. Sigalas, M. Kafesaki, E.N. Economou, Phononic crystals and elastodynamics: Some relevant points, AIP Adv. 4 (2014) 1–18. doi:10.1063/1.4904406.
[53] R. Ahmed, F. Mir, S. Banerjee, A review on energy harvesting approaches for renewable energies from ambient vibrations and acoustic waves using piezoelectricity, Smart Mater. Struct. 26 (2017) 085031. doi:10.1088/1361-665X/aa7bfb.
[54] Z. Liu, X. Zhang, Y. Mao, Y.Y. Zhu, Z. Yang, C.T. Chan, P. Sheng, Locally resonant sonic materials, Science. (2000). doi:10.1126/science.289.5485.1734.
[55] M. Carrara, M.R. Cacan, J. Toussaint, M.J. Leamy, M. Ruzzene, A. Erturk, Metamaterial-inspired structures and concepts for elastoacoustic wave energy harvesting, Smart Mater. Struct. 22 (2013). doi:10.1088/0964-1726/22/6/065004.
[56] T. Miyashita, Sonic crystals and sonic wave-guides, Meas. Sci. Technol. 16 (2005) 47–63. doi:10.1088/0957-0233/16/5/R01.
[57] A. Gupta, A review on sonic crystal, its applications and numerical analysis techniques,

Acoust. Phys. 60 (2014) 223–234. doi:10.1134/S1063771014020080.
[58] P. Sheng, X.X. Zhang, Z. Liu, C.T. Chan, Locally resonant sonic materials, Phys. B Condens. Matter. 338 (2003) 201–205. doi:10.1016/S0921-4526(03)00487-3.
[59] L.-Y. Wu, L.-W. Chen, C.-M. Liu, Acoustic energy harvesting using resonant cavity of a sonic crystal, Appl. Phys. Lett. 95 (2009) 013506. doi:10.1063/1.3176019.
[60] W.C. Wang, L.Y. Wu, L.W. Chen, C.M. Liu, Acoustic energy harvesting by piezoelectric curved beams in the cavity of a sonic crystal, Smart Mater. Struct. 19 (2010). doi:10.1088/0964-1726/19/4/045016.
[61] S. Qi, M. Oudich, Y. Li, B. Assouar, Acoustic energy harvesting based on a planar acoustic metamaterial, Appl. Phys. Lett. 108 (2016). doi:10.1063/1.4954987.
[62] K. Song, S.H. Lee, K. Kim, S. Hur, J. Kim, Emission enhancement of sound emitters using an acoustic metamaterial cavity, Sci. Rep. 4 (2014) 1–6. doi:10.1038/srep04165.
[63] K. Song, K. Kim, S. Hur, J.H. Kwak, J. Park, J.R. Yoon, J. Kim, Sound pressure level gain in an acoustic metamaterial cavity, Sci. Rep. 4 (2014) 4–9. doi:10.1038/srep07421.
[64] Z. Liang, J. Li, Extreme acoustic metamaterial by coiling up space, Phys. Rev. Lett. 108 (2012) 1–4. doi:10.1103/PhysRevLett.108.114301.
[65] H. Guo, Y. Wang, X. Wang, C. Xu, Investigation on acoustic energy harvesting based on quarter-wavelength resonator phononic crystals, Adv. Mech. Eng. 10 (2018) 168781401774807. doi:10.1177/1687814017748077.
[66] M. Yuan, Z. Cao, J. Luo, R. Ohayon, Acoustic metastructure for effective low frequency acoustic energy harvesting, J. Low Freq. Noise, Vib. Act. Control. (2018). doi:10.1177/1461348418794832.
[67] C.J. Naify, C.M. Chang, G. McKnight, S. Nutt, Transmission loss and dynamic response of membrane-type locally resonant acoustic metamaterials, J. Appl. Phys. 108 (2010). doi:10.1063/1.3514082.
[68] Z. Yang, J. Mei, M. Yang, N.H. Chan, P. Sheng, Membrane-type acoustic metamaterial with negative dynamic mass, Phys. Rev. Lett. 101 (2008) 1–4. doi:10.1103/PhysRevLett.101.204301.
[69] M. Javadi, A. Heidari, S. Darbari, Realization of enhanced sound-driven CNT-based triboelectric nanogenerator, utilizing sonic array configuration, Curr. Appl. Phys. 18 (2018) 361–368. doi:10.1016/j.cap.2018.01.018.
[70] M.M.J. Treacy, T.W. Ebbesen, J.M. Gibson, Exceptionally high Young's modulus observed for individual carbon nanotubes, Nature. (1996). doi:10.1038/381678a0.
[71] F.R. Fan, Z.Q. Tian, Z. Lin Wang, Flexible triboelectric generator, Nano Energy. 1 (2012) 328–334. doi:10.1016/j.nanoen.2012.01.004.
[72] J. Yang, J. Chen, Y. Yang, H. Zhang, W. Yang, P. Bai, Y. Su, Z.L. Wang, Broadband vibrational energy harvesting based on a triboelectric nanogenerator, Adv. Energy Mater. 4 (2014) 1–9. doi:10.1002/aenm.201301322.
[73] H. Wang, M. Shi, K. Zhu, Z. Su, X. Cheng, Y. Song, X. Chen, Z. Liao, M. Zhang, H. Zhang, High performance triboelectric nanogenerators with aligned carbon nanotubes, Nanoscale. 8 (2016) 18489–18494. doi:10.1039/c6nr06319e.
[74] M. Oguntoye, M. Johnson, L. Pratt, N.S. Pesika, Triboelectricity Generation from Vertically Aligned Carbon Nanotube Arrays, ACS Appl. Mater. Interfaces. 8 (2016) 27454–

27457. doi:10.1021/acsami.6b11457.
[75] A. Yang, P. Li, Y. Wen, C. Lu, X. Peng, J. Zhang, W. He, Enhanced acoustic energy harvesting using coupled resonance structure of sonic crystal and helmholtz resonator, Appl. Phys. Express. 6 (2013) 4–7. doi:10.7567/APEX.6.127101.
[76] A. Yang, P. Li, Y. Wen, C. Yang, D. Wang, F. Zhang, J. Zhang, High-Q cross-plate phononic crystal resonator for enhanced acoustic wave localization and energy harvesting, Appl. Phys. Express. 8 (2015). doi:10.7567/APEX.8.057101.
[77] F.U. Khan, Izhar, Hybrid acoustic energy harvesting using combined electromagnetic and piezoelectric conversion, Rev. Sci. Instrum. 87 (2016). doi:10.1063/1.4941840.
[78] V. Nguyen, R. Yang, Effect of humidity and pressure on the triboelectric nanogenerator, Nano Energy. 2 (2013) 604–608. doi:10.1016/j.nanoen.2013.07.012.
[79] G. Zhu, B. Peng, J. Chen, Q. Jing, Z. Lin Wang, Triboelectric nanogenerators as a new energy technology: From fundamentals, devices, to applications, Nano Energy. 14 (2015) 126–138. doi:10.1016/j.nanoen.2014.11.050.
[80] N. Cui, L. Gu, J. Liu, S. Bai, J. Qiu, J. Fu, X. Kou, H. Liu, Y. Qin, Z.L. Wang, High performance sound driven triboelectric nanogenerator for harvesting noise energy, Nano Energy. 15 (2015) 321–328. doi:10.1016/j.nanoen.2015.04.008.
[81] J. Liu, N. Cui, L. Gu, X. Chen, S. Bai, Y. Zheng, C. Hu, Y. Qin, A three-dimensional integrated nanogenerator for effectively harvesting sound energy from the environment, Nanoscale. 8 (2016) 4938–4944. doi:10.1039/c5nr09087c.
[82] Z. Zhou, W. Qin, P. Zhu, Harvesting acoustic energy by coherence resonance of a bi-stable piezoelectric harvester, Energy. 126 (2017) 527–534. doi:10.1016/j.energy.2017.03.062.
[83] H.-M. Noh, Acoustic energy harvesting using piezoelectric generator for railway environmental noise, Adv. Mech. Eng. 10 (2018) 168781401878505. doi:10.1177/1687814018785058.
[84] Y. Wang, X. Zhu, T. Zhang, S. Bano, H. Pan, L. Qi, Z. Zhang, Y. Yuan, A renewable low-frequency acoustic energy harvesting noise barrier for high-speed railways using a Helmholtz resonator and a PVDF film, Appl. Energy. 230 (2018) 52–61. doi:10.1016/j.apenergy.2018.08.080.

Fig. 1.

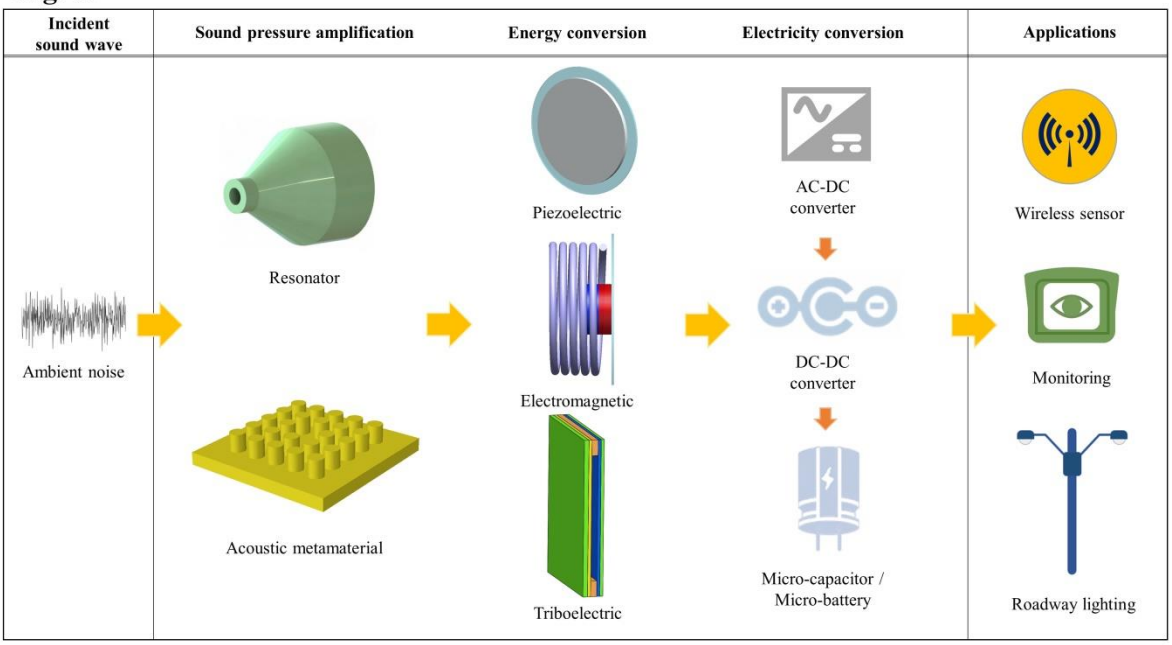

Fig. 2.

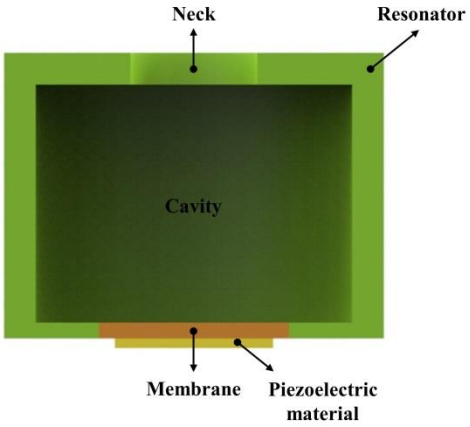

Fig. 3.

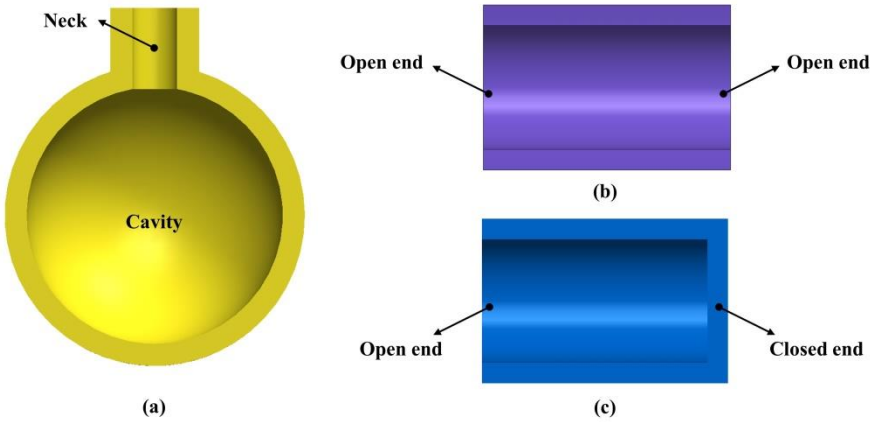

Fig. 4.

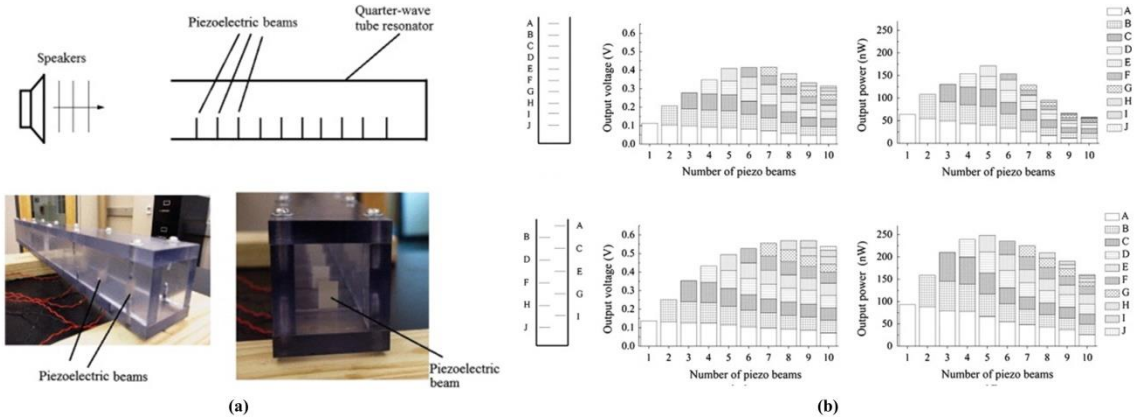

Fig. 5.

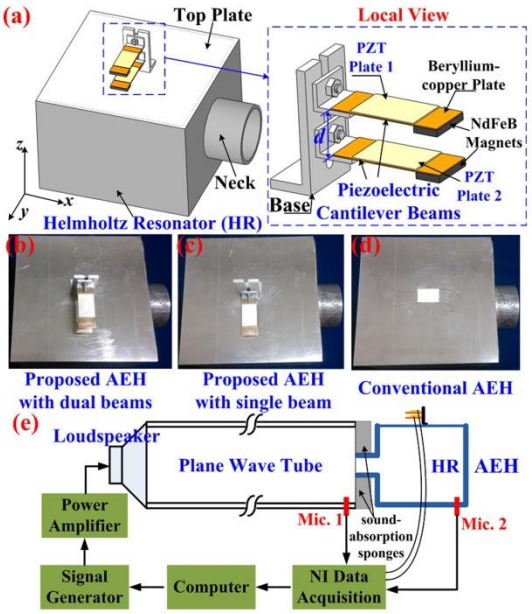

Fig. 6.

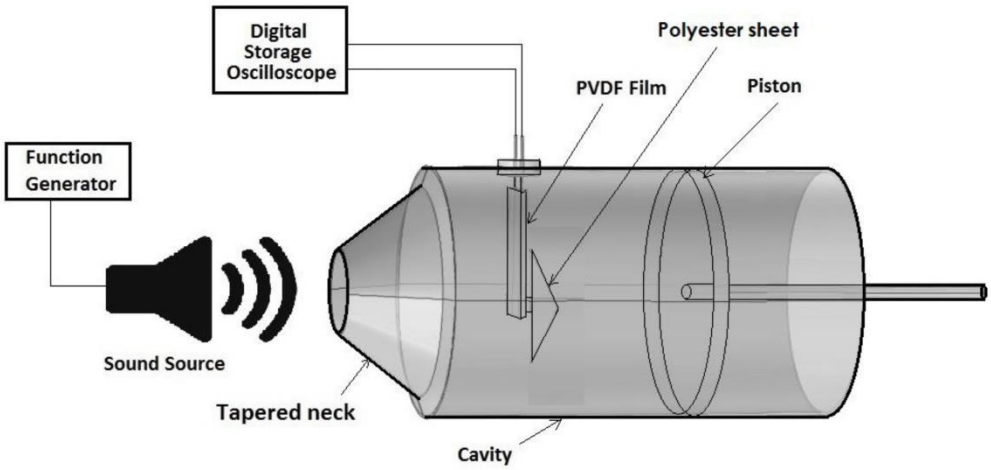

Fig. 7.

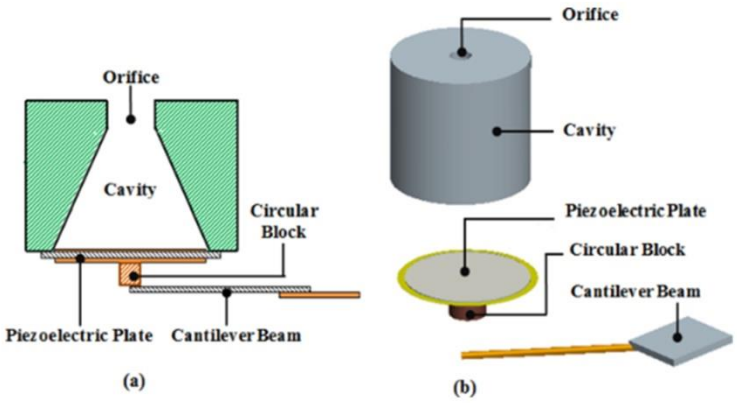

Fig. 8.

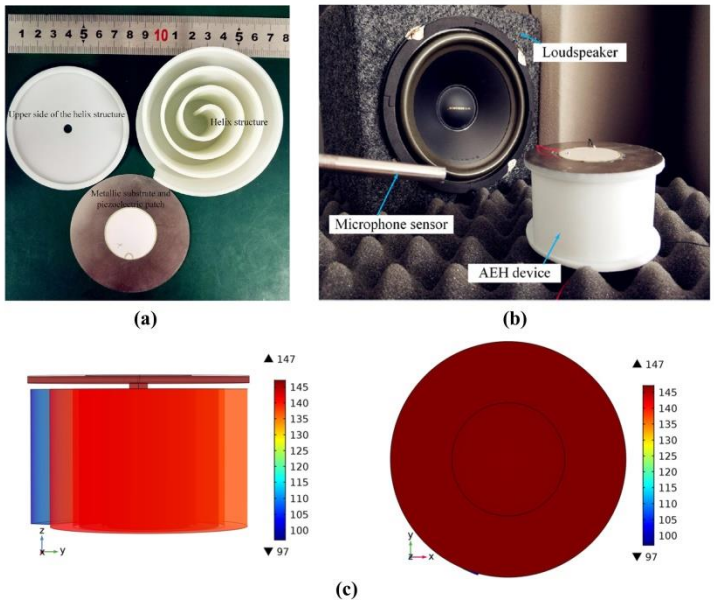

Fig. 9.

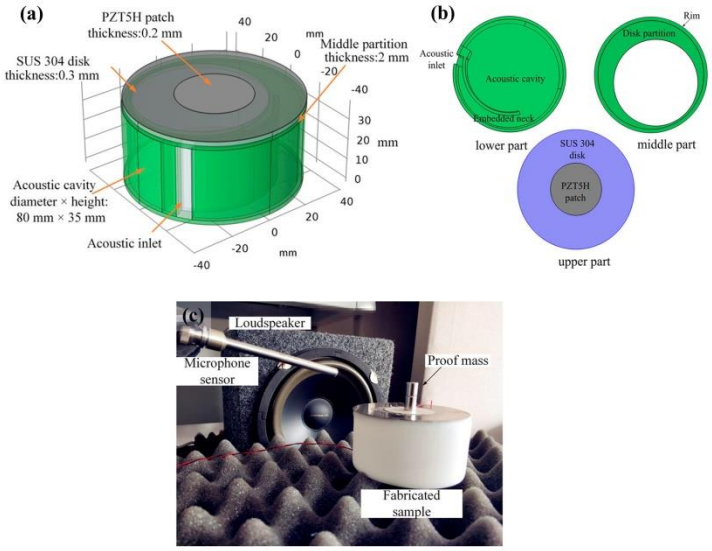

Fig. 10.

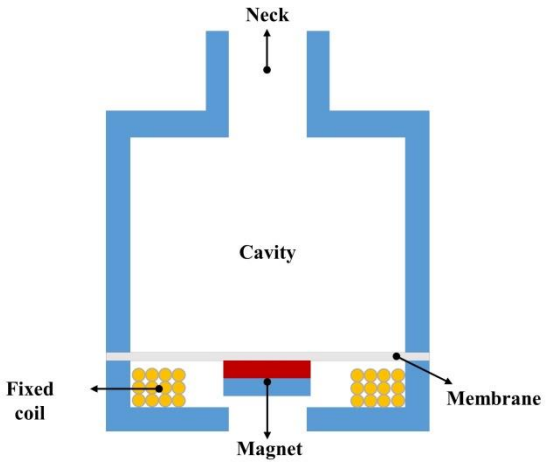

Fig. 11.

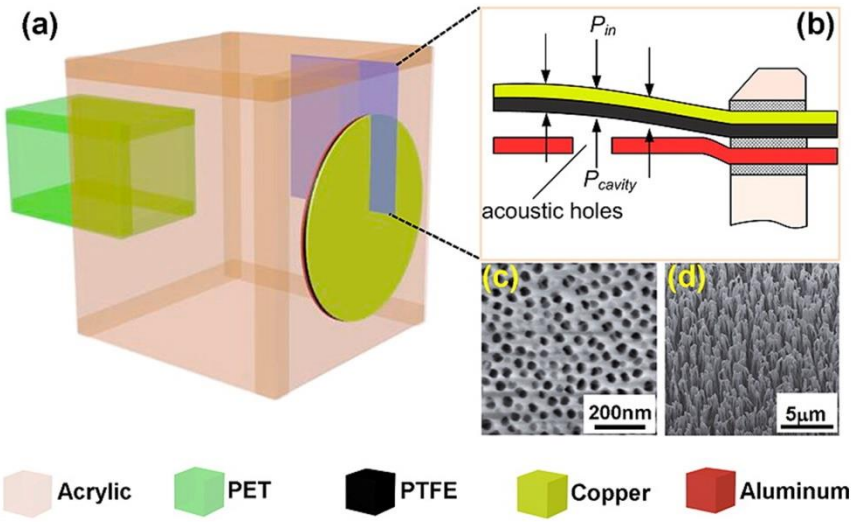

Fig. 12.

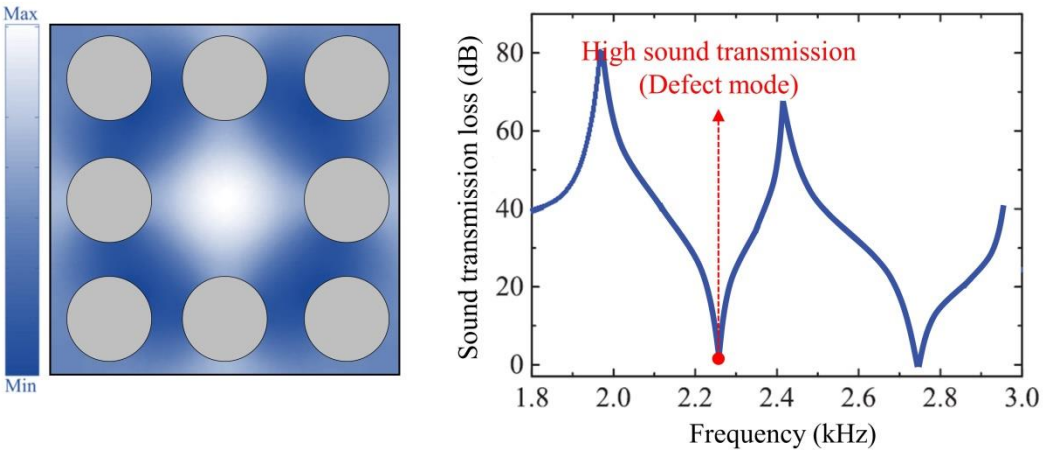

(a) **(b)**

Fig. 13.

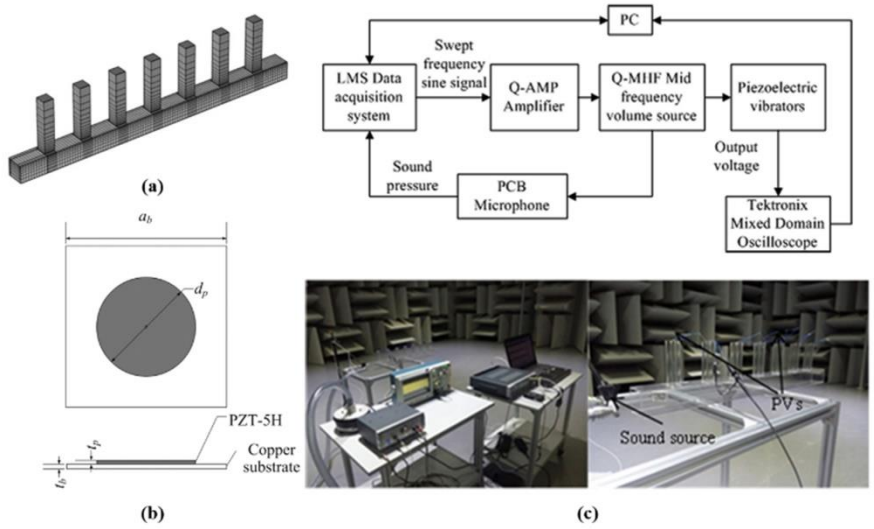

Fig. 14.

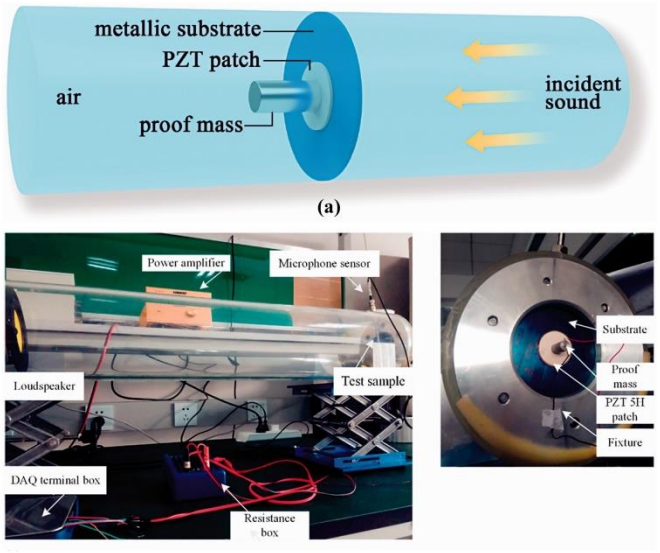

Fig. 15.

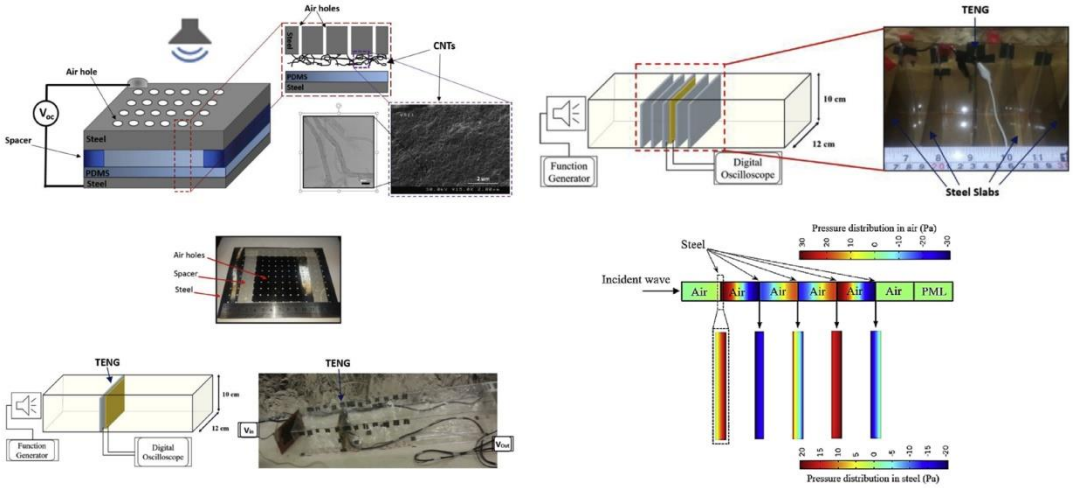

(a) **(b)**

Fig. 16.

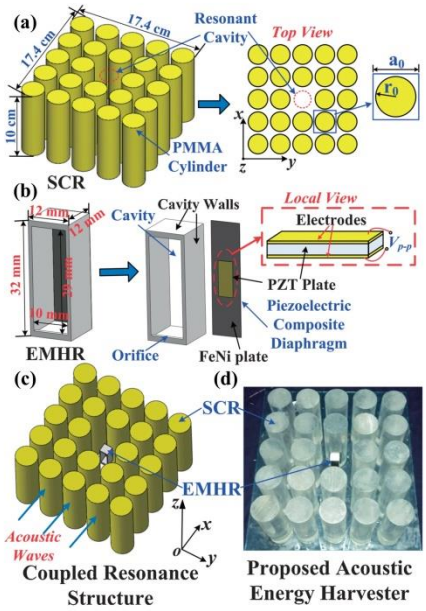

Fig. 17.

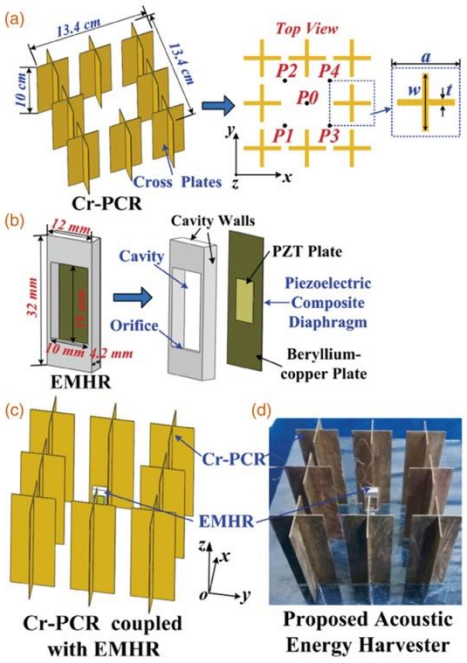

Fig. 18.

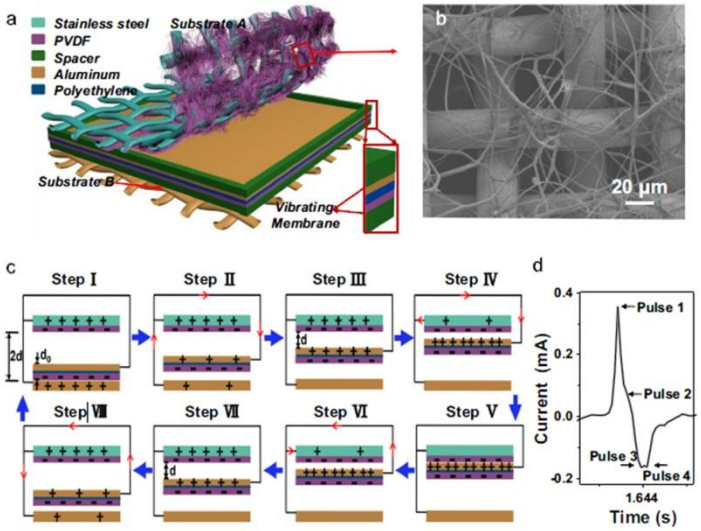

Fig. 19.

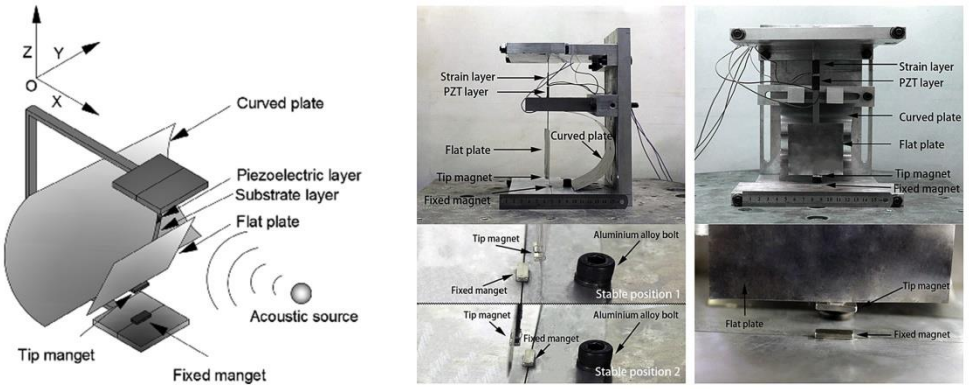

(a) **(b)**

Table 1. Sound pressure level of various sound sources.

Sound energy source	Sound pressure level (dB)
Jet engine at 1 m	150
Stun grenade	158 - 172
Simple open-ended thermoacoustic device	176
Car air conditioning system	71.9
Inside airplane	86
Auditory threshold at 1 kHz	0
Normal conversation	40 - 60
Threshold of pain	130 - 140
Rustling of leaves	20
Quiet room	40
Sonic boom	110
Traffic on a busy roadway at 10 m	80 - 90
Jack hammer	100

Table 2. Summary of resonator based sound energy harvesters.

Type	Reference	Brief summary	Device size (cm^3)	SPL (dB)	Load resistance (Ω)	Resonant frequency (Hz)	Voltage (V)	Power output (μW)
Piezoelectric	Horowitz *et al* [35]	A MEMS piezoelectric sound energy harvester	2.445	149	982.9	13568	–	6×10^{-6}
	Li *et al* [30,36]	Sound energy harvester using PZT piezoelectric beam array in a quarter-wavelength resonator	840	110	19371	199	15.689	12697
	Li *et al* [31]	Sound energy harvester using PVDF piezoelectric beam array in a quarter-wavelength resonator	1500	110	1×10^{6}	146	1.48	2.2
	Yang *et al* [27]	A broadband sound energy harvester using dual PZT piezoelectric beams located on the top of Helmholtz resonator	3972.22	100	38000	170 – 206	–	137 – 1430
	Pillai *et al* [37]	Taped neck Helmholtz resonator based sound energy harvester with a flexible triangular foil	2477.78	103	–	99	0.842	–
	Izhar *et al* [39]	3 DOF sound energy harvester using a Helmholtz resonator and a piezoelectric plate with a circular block and a cantilever beam	13.12	130	1000	1453 – 1542, 1710 – 1780, 1848 – 1915	0.461	214.23
	Yuan *et al* [41]	Sound energy harvester using a helix structure	251	100	11000	175	0.283	7.3

	Yuan *et al* [25]	Sound energy harvester based on a spiral Helmholtz resonator	200	100	10000 6000	217 (acoustic resonance) 341 (mechanical resonance)	0.522 0.622	27.2 64.4
Electromagnetic	Khan *et al* [46]	Electromagnetic based sound energy harvester	14.728	125	52	143	0.319	1960
	Lai *et al* [47]	Micro-scale electromagnetic sound energy harvester	0.009	–	–	470	0.24×10^{-3}	–
	Izhar *et al* [48]	Electromagnetic sound energy harvester with a cone shaped cavity	43.1	100	147	330.3	0.182	212
Triboelectric	Yang *et al* [49]	Triboelectric sound energy harvester by utilizing a Helmholtz resonator	570	110	6×10^{6}	240	47.5	376

Table 3. Summary of acoustic metamaterial based sound energy harvesters

Type	Reference	Brief summary	Device size (cm^3)	SPL (dB)	Load resistance (Ω)	Resonant frequency (Hz)	Voltage (V)	Power output (μW)
Piezoelectric	Wu *et al* [59]	Sound energy harvesting using resonant cavity of a sonic crystal	9236.28	45	3900	4200	17.7×10^{-3}	40×10^{-3}
	Yang *et al* [60]	Sound energy harvesting by piezoelectric curved beams in the cavity of a sonic crystal	9236.28	–	15000	4210	23.6×10^{-3}	37×10^{-3}
	Qi *et al* [61]	Sound energy harvester based on a defected acoustic metamaterial with a circular piezoelectric material	5.964	100	38000	2257.5	1.3	8.8
	Sun *et al* [44]	Sound energy harvester using a doubly coiled-up acoustic metamaterial cavity	676	100	20000	600	0.2585	0.345
	Guo *et al* [65]	Sound energy harvester based on a quarter-wavelength resonator phononic crystal	2870	94	5100	710	17×10^{-3}	56.67×10^{-3}
	Yuan *et al* [66]	Sound energy harvester based on acoustic metastructure with a metallic substrate, a piezoelectric patch and proof mass	2.133	114	8100	155	1.304	210
Triboelectric	Javadi *et al* [69]	1D sonic array based triboelectric sound energy harvester with CNTs	6.9	–	1×10^{6}	4240	0.22	40×10^{-3}

Table 4. Summary of other kinds of sound energy harvesters

Type	Reference	Brief summary	Device size (cm^3)	SPL (dB)	Load resistance (Ω)	Resonant frequency (Hz)	Voltage (V)	Power output (μW)
Piezoelectric	Yang *et al* [75]	Sound energy harvesting using coupled resonance structure of sonic crystal and Helmholtz resonator	3027.6	110	4400	5545	3.89	429
	Yang *et al* [76]	Sound energy harvesting using coupled resonance structure of cross-plate phononic crystal and Helmholtz resonator	1795.6	100	4000	6975	4.3	578
	Zhou *et al* [82]	A bi-stable sound energy harvester for harvesting broadband noise energy	23.2	105	–	almost 0	0.4	–
Piezoelectric, Electromagnetic	Khan *et al* [77]	Sound energy harvester using combined electromagnetic and piezoelectric conversion method	21.208	130	1000 (piezoelectric) 114 (electromagnetic)	2100	0.443 0.038	49 3.16
Triboelectric	Cui *et al* [80]	Triboelectric sound energy harvester with two substrates and one vibrating membrane	1.05	114	100	160	70	2.02×10^{3}
	Liu *et al* [81]	An integrated triboelectric nanogenerator with a three-dimensional structure	5.28	100.5	100	200	232	48.87×10^{3}

Highlights

- This paper summarizes the basic principles of sound energy harvesters and its state-of-the-art researches.
- We mainly classified the sound energy harvesters as sound pressure amplification methods such as using a resonator and using an acoustic metamaterial.
- The comparison and discussion of the reported sound energy harvesters are provided according to sound pressure amplification, transduction mechanism, device size, incident sound pressure level, load impedance, resonant frequency, and generated power.